Surface-Initiated Polymerization of Thiophene and Pyrrole Monomers on Poly(terthiophene) Films and Oligothiophene Monolayers

Gianni Zotti,* Sandro Zecchin, and Barbara Vercelli

Istituto per l'Energetica e le Interfasi, Consiglio Nazionale delle Ricerche c.o Stati Uniti 4, 35127 Padova, Italy

Anna Berlin and Sara Grimoldi

Istituto di Scienze e Tecnologie Molecolari, Consiglio Nazionale delle Ricerche, via C.Golgi 19, 20133 Milano, Italy

Lambert Groenendaal

Agfa Gevaert N.V., R&D Materials Research - Chemistry Department, Septelaan 27, B-2640 Mortsel, Belgium

Renzo Bertoncello

Dip. di Scienze Chimiche, Università di Padova, via Loredan 4, 35131 Padova, Italy

Marco Natali

Istituto di Chimica Inorganica e delle Superfici, Consiglio Nazionale delle Ricerche c.o Stati Uniti 4, 35127 Padova, Italy

Received February 10, 2005. Revised Manuscript Received April 18, 2005

Thin polyterthiophene films and oligothiophene-based self-assembled monolayers (SAMs) on indium tin oxide (ITO) and gold electrodes have been coupled with different pyrrole- and thiophene-based monomers (heterocoupling). Since the corresponding homopolymers are soluble in the electrochemical medium, only the surface-coupled polymer remains on the electrode and is detected. The method when applied to monolayers allows the formation of nanometer-size layers of polyconjugated polymers with nominally normal orientation of the chain to the surface. Thin films and SAMs were characterized before and after coupling by cyclic voltammetry, UV−vis and IR reflection absorption spectroscopy, and X-ray photoelectron spectroscopy. Microcontact printing on gold and ITO surfaces resulted in patterns for which atomic force microscopy evidenced strong height enhancement after heterocoupling.

1. Introduction

Self-assembled monolayers (SAMs)[1] may be initiator systems for the preparation of uniform and densely grafted polymer brushes.[2−5] One important aspect offered by this method is the possibility of controlling the position of the initiator sites within the monolayer. Controlling the grafting density of the resulting polymer brush by, e.g., mixed SAMs, allows the preparation of two-component gradients or the construction of complex spatial structures. The latter can be formed by, e.g., microcontact printing, for structures ranging from hundreds of nanometers to several hundred micrometers.

A combination of directed deposition of functionalized areas of SAMs and consecutive surface-initiated polymerization allows a superior control of pattern formation and amplification of the patterns by creating polymer-brush layers at predefined sites. Surface defects and topological features of the substrate are covered by the polymer brush producing a higher contrast between chemical and physical properties of functionalized and unfunctionalized areas which allows the production of surfaces for many technological applications.

The use of polyconjugated oligomers or polymers in SAMs is at present considered promising for optoelectronic applications and for molecular electronics.[6,7] In particular their

* To whom correspondence may be addressed. Tel.: (39) 049-829-5868. Fax: (39) 049-829-5853. E-mail: g.zotti@ieni.cnr.it.

(1) Kumar, A.; Abbott, N.L.; Kim, E.; Biebuick, H.A.; Whitesides, G.M. *Acc. Chem. Res.* **1995**, *28*, 219; Ulman, A. *Chem. Rev.* **1996**, *96*, 1533.
(2) Shah, R.R.; Merreceyes, D.; Husemann, M.; Rees, I.; Abbott, N.L.; Hawker, C.J.; Hedrick, J.L. *Macromolecules* **2000**, *33*,597.
(3) Zhou, F.; Liu, W.; Hao, J.; Xu, T.; Chen, M.; Xue, Q. *Adv. Funct. Mater.* **2003**, *13*, 938.
(4) Schmelmer, U.; Jordan, R.; Geyer, W.; Eck, W.; Golzhauser, A.; Grunze, M.; Ulman, A. *Angew. Chem., Int. Ed.* **2003**, *42*, 559.
(5) (a) Biesalski, M.; Ruhe, J. *Macromolecules* **2004**, *37*, 2196. (b) Ma, H.; Hyun, J.; Stiller, P.; Chilkoti, A. *Adv. Mater.* **2004**, *16*, 338.
(6) Fabre, B.; Wayner, D.D. M. *Langmuir* **2003**, *19*, 7145.
(7) Liang, Z.; Rackaitis, M.; Li, K.; Manias, E.; Wang, Q. *Chem. Mater.* **2003**, *15*, 2699.

10.1021/cm050300l CCC: $30.25
Published on Web 06/07/2005

Chart 1

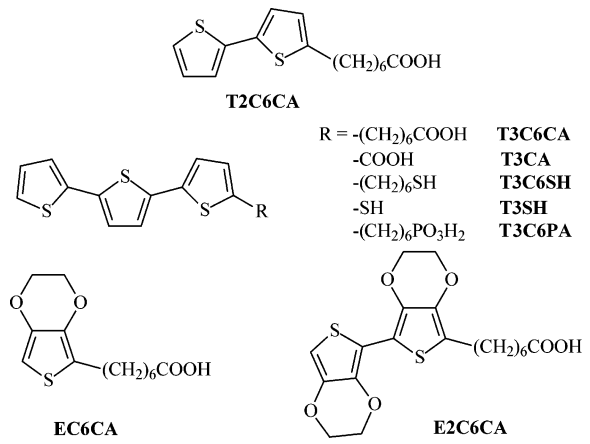

reactivity to polymers grafting, i.e., the brush-forming step, has been much investigated. The topic of SAMs of polyconjugated (mainly pyrrole- and thiophene-based) oligomers has been reviewed in a feature article covering the literature to 1998.[8] Among subsequent reports we may mention SAMs of bithiophene,[9] terthiophene,[10,11] and tetrathiophene,[12] which were directly linked to a gold surface via thiol ends. More recently tripod-shaped thiols have been used for the production of more complex and stable oligothiophene SAMs for use in light-emitting diodes (LEDs).[13] Particularly interesting is that a SA layer of quaterthiophene−dodecanethiol was coupled with an alkyl-substituted terthiophene to form a heptathiophene layer[12] as a model system for polymer grafting via coupling.

An interesting extension of the coupling of SAMs with parent monomers (homocoupling) is their coupling to different monomers (heterocoupling). In fact sequential solid-state polymerization is a new method for the production of selected oligomeric sequences which has been applied for, e.g., the synthesis of oligothiophene− or oligophenylene−ethynylenes[14] or to the production of brush electrodes with conjugated hair.[15,16] Anodic heterocoupling is in any case a yet unexplored topic.

In our aim at the production of such type of electrodes from monolayers, we have investigated the coupling of thiophene-based (Chart 1) monolayers on indium tin oxide (ITO) and gold electrodes with different pyrrole- and thiophene-based molecules, both monomeric and dimeric (Chart 2). The corresponding homopolymers are soluble in the electrochemical medium so that only the surface-coupled

Chart 2

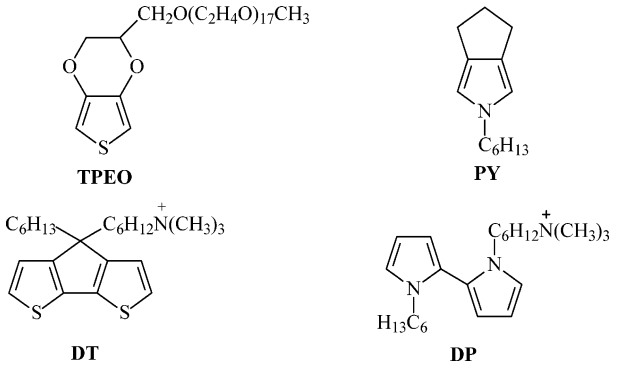

polymer remains and is detected, i.e., a clean (free of unconnected polymer) polymer brush electrode is in principle obtained. The oligothiophene-tailed adsorbates bear carboxyl or phosphonate heads for ITO grafting whereas thiol heads are used for gold.

The overall process is illustrated in Scheme 1. The method allows the formation of nanometer-size layers of polyconjugated polymers with nominally normal orientation of the chain to the surface. This also makes possible the formation of stable layers of otherwise soluble polymers.

SAMs were characterized before and after coupling by cyclic voltammetry (CV), UV−vis, IR reflection absorption spectroscopy (IRRAS), and X-ray photoelectron spectroscopy (XPS). Microcontact printing on gold and ITO surfaces resulted in patterns for which atomic force microscopy (AFM) evidenced strong height enhancement by heterocoupling.

In this report we present also as an introductory section the above-mentioned modifications performed on thin films of polyterthiophene (PTT). This polymer is in fact a sexithiophene which upon oxidation forms reactive radical cations able to self-polymerize.[17,18] The present approach allows the comparison of different reactivities to heterocoupling starting from a bulk polymer film.

2. Experimental Section

2.1. Chemicals and Reagents. All melting points are uncorrected. All reactions of air- and water-sensitive materials were performed under nitrogen. Air- and water-sensitive solutions were transferred with double-ended needles. The solvents used in the reactions (Fluka) were absolute and stored over molecular sieves. Acetonitrile was reagent grade (Uvasol, Merck) with a water content <0.01%. The supporting electrolyte tetrabutylammonium perchlorate (Bu_4NClO_4) and all other chemicals were reagent grade and used as received.

The following compounds were prepared according to literature procedures: 7-(2,2′-bithien-5-yl)heptanoic acid (T2C6CA),[19] 7-(2,2′:5′,2"-terthien-5-yl)heptanoic acid (T3C6CA),[19] 2,2′:5′,2″-terthiophene-5-carboxylic acid (T3CA),[20] 6-(2,2′:5′,2"-terthien-5-yl)hexane-1-thiol (T3C6SH),[21] 5-bromo-2,2′:5′,2″-terthiophene,[22] 5-(6-bromo-

(8) Berlin, A.; Zotti, G. *Macromol. Rapid Comm.* **2000**, *21*, 301.
(9) Tour, J.M.; Jones, L.; Pearson, D.L.; Lamba, J.J. S.; Burgin, T.P.; Whitesides, G.M.; Allara, D.L.; Parikh, A.N.; Atre, S.V. *J. Am. Chem. Soc.* **1995**, *117*, 9529.
(10) Liedberg, B.; Yang, Z.; Engquist, I.; Wirde, M.; Gelius, U.; Gotz, G.; Bauerle, P.; Rummel, R.M.; Ziegler, C.; Gopel, W. *J. Phys. Chem. B* **1997**, *101*, 5951.
(11) Michalitsch, R.; Kassim, E. I.; Yassar, A.; Lang, P.; Garnier, F. *J. Electroanal. Chem.* **1998**, *457*, 129.
(12) Nogues, C.; Lang, P.; Rei Vilar, M.; Desbat, B.; Buffeteau, T.; El-Kassmi, A.; Garnier, F. *Colloids Surf., A.* **2002,***198*−*200*, 577.
(13) Zhu, L.; Tang, H.; Harima, Y.; Yamashita, K.; Aso, Y.; Otsubo, T. *J. Mater. Chem.* **2002**, *12*, 2250.
(14) Tour, J.M. *Acc. Chem. Res.* **2000**, *33*, 791.
(15) Rosink, J.J. W. M.; Blaw, M.A.; Geeligs, L.J.; Van der Drift, E.; Rousseeuw, B.A. C.; Radelaar, S. *Langmuir*, **2000**, *16*, 4547.
(16) Zotti, G.; Randi, A.; Destri, S.; Porzio, W.; Schiavon, G. *Chem. Mater.* **2002**, *14*, 4550.
(17) (a) Zotti, G.; Schiavon, G. *Synth. Met.* **1990**, *39*, 183. (b) Zotti, G.; Schiavon, G.; Berlin, A.; Pagani, G. *Chem. Mater.* **1993**, *5*, 620.
(18) Meerholz, K.; Heinze, J. *Electrochim. Acta* **1996**, *41*, 1839.
(19) Berlin, A.; Zotti, G.; Schiavon, G.; Zecchin, S. *J. Am. Chem. Soc.* **1998**, *120*, 13453.
(20) Kagan, J.; Arora, S.K.; Üstünol, A. *J. Org. Chem.* **1983**, *48*, 4076.
(21) Michalitsch, R.; Lang, P; Yassar, A.; Nauer, G.; Garnier, F. *Adv. Mater.* **1997**, *9*, 321.

Scheme 1

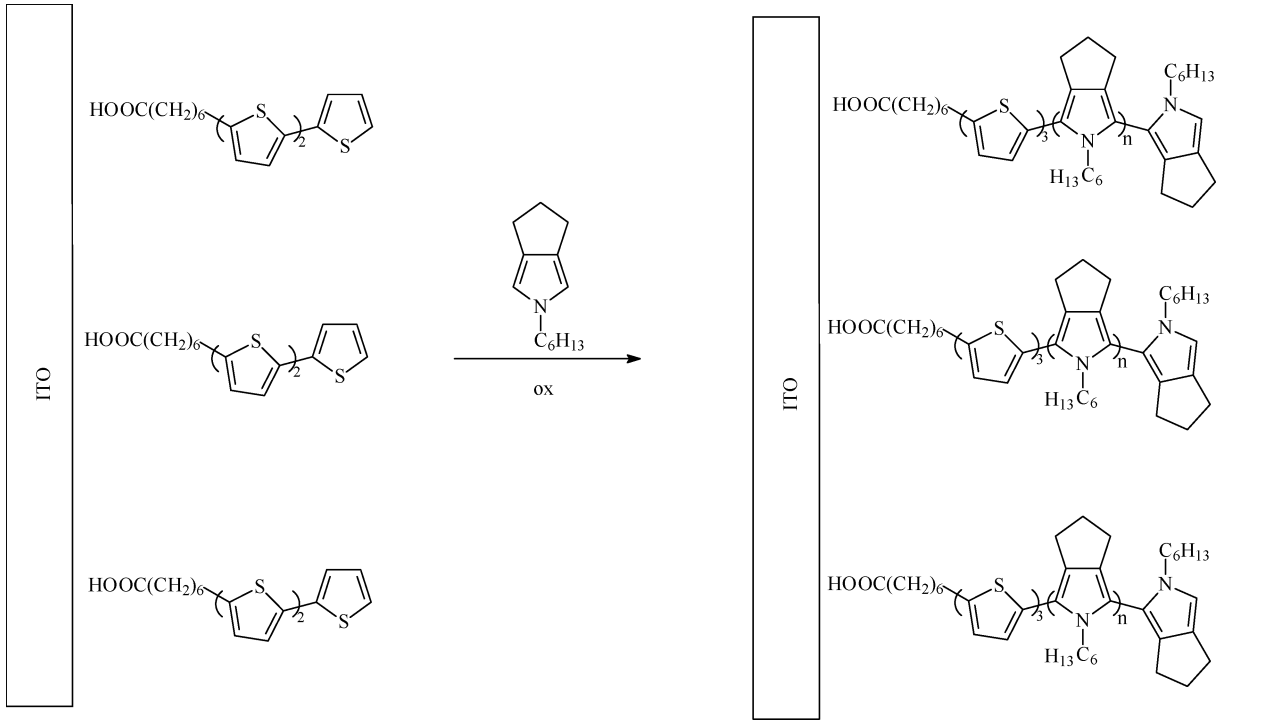

hexyl)-2,2′:5′,2"-terthiophene,[19] 2-(tributylstannyl)-3,4-(ethylenedioxy)thiophene,[23] poly(ethylene oxide)-modified (2,3-dihydrothieno[3,4−b1,4]dioxin-2-yl)-methanol (M_w = ca. 890) (TPEO),[24] *N*-hexyl-cyclopenta[c]pyrrole (PY),[25] {6-(4-hexyl-4*H*-cyclopenta-[2,1-b:3,4-b′]dithiophen-4yl)hexyl}trimethylammonium perchlorate (DT),[26] [6-(1′-hexyl-1′*H*-[2,2′]bipyrrol-1-yl)-hexyl]trimethylammonium tetrafluroborate (DP).[27]

^{1}H and ^{13}C NMR spectra were recorded on a Bruker FT 300 (300 MHz for ^{1}H); chemical shift values are given in parts per million.

2,2′:5′,2″-Terthiophene-5-thiol (T3SH). BuLi (1.6 M in hexane, 0.48 mL, 0.76 mmol) was added dropwise to a solution of 5-bromo-2,2′:5′:2″-terthiophene (250 mg, 0.76 mmol) in THF (20 mL) at −78 °C. After 30 min of stirring, sublimated sulfur (24 mg, 0.76 mmol) was added, and the reaction mixture was stirred for 3 h at the same temperature. NaOH (1 M, 5 mL) was added, and the aqueous layer was acidified with a 2 M solution of HCl and extracted with hexane. The organic phase was washed with water, dried (Na_2SO_4), and the solvent evaporated at reduced pressure to give the title compound as an orange solid (116 mg, 52% yield). Anal. Calcd for $C_{12}H_8S_4$: C, 51.41; H, 2.85%. Found: C, 51.32; H, 2.73%. ^{1}H NMR ($CDCl_3$): δ 3.57 (s, 1H), 7.01 (m, 5H), 7.19 (m, 2H). MS, *m*/*e* 280 ($M^{\bullet}$+).

Diethyl 6-(2,2′:5′,2″-Terthien-5-yl)hexylphosphonate. A mixture of 5-(6-bromohexyl-2,2′:5′,2″-terthiophene (410 mg, 0,99 mmol) and triethyl phosphite (174 mg, 1.05 mmol) was stirred for 6 h at 160 °C. Flash chromatography (silica gel, CH_2Cl_2/AcOEt 8:2) of the obtained product afforded the title compound (334 mg, 71% yield). Anal. Calcd for $C_{22}H_{29}O_3PS_3$: C, 56.42; H, 6.19%. Found: C, 56.35; H, 6.03%. ^{1}H NMR ($CDCl_3$): δ 1.32 (t, 6H), 1.35 (m, 4H), 1.66 (m, 4H), 2.79 (m, 2H), 4.09 (m, 6H), 6.68 (d, 1H), 7.01 (m, 4H), 7.15 (m, 1H), 7.20 (m, 2H).

6-(2,2′:5′,2″-Terthien-5-yl)hexylphosphonic acid (T3C6PA). Trimethylbromosilane (278 mg, 1.82 mmol) was added dropwise to a solution of diethyl 6-(2,2′:5′,2″-terthien-5-yl)hexylphosphonate (334 mg, 0.71 mmol) in CH_2Cl_2 (5 mL), and the resulting solution was stirred for 6 h. The solvent and excess trimethylbromosilane were evaporated at reduced pressure leaving a yellow solid which was shown to be the sylil ester by ^{1}H NMR. The sylil ester was dissolved in methanol (125 mL), and the solution was stirred for 5 min, followed by removal of methanol under reduced pressure. The hydrolysis procedure was repeated three times yielding the title compound as a yellow solid (295 mg, 100% yield), mp 142−145 °C. Anal. Calcd for $C_{18}H_{21}O_3PS_3$: C, 52.43; H, 5.09%. Found: C, 52.37; H, 5.15%. ^{1}H NMR (d_6-DMSO): δ 1.25−1.61 (m, 8H), 1.63 (t, 2H), 2.79 (m, 2H), 6.81 (d, 1H), 7.09 (m, 1H), 7.13 (m, 1H), 7.16 (m, 1H), 7.23 (m, 1H), 7.31 (m, 1H), 7.52 (d, 1H). ^{31}P NMR (d_6-DMSO) δ 32.95 vs 85% H_3PO_4. MS, *m*/*e* 412 ($M^{\bullet}$+).

2-(6-Bromohexyl)-3,4-(ethylenedioxy)thiophene. BuLi (1.6 M in hexane, 8.9 mL, 14.21 mmol) was added dropwise to a stirred solution of 3,4-(ethylenedioxy)thiophene (2,00 mg, 14,21 mmol) in THF (30 mL) keeping the temperature at −78 °C. The solution was stirred for 30 min and then added dropwise to a solution of 1,6-dibromohexane (3.53 g, 14,49 mmol) in THF (20 mL) keeping the temperature at −78 °C. After 24 h of stirring at room temperature, the reaction mixture was poured into water and extracted with ether. The organic phase was dried (Na_2SO_4), and the solvent evaporated. Flash chromatography (silica gel, petroleum ether/ether) of the residue afforded the title compound (2.25 g, 52% yield) as an oil. Anal. Calcd for $C_{12}H_{17}BrO_2S$: C, 47.24; H, 5.57%. Found: C, 47.15; H, 5.51%. ^{1}H NMR ($CDCl_3$): δ 1.45 (m, 4H), 1.59 (m, 2H), 1.89 (m, 2H), 2.63 (t, 2H), 3.42 (t, 2H), 4.16 (s, 4H), 6.13 (s, 1H).

7-[3,4-(Ethylenedioxy)thien-2-yl]heptanenitrile. A mixture of 2-(6-bromohexyl)-3,4-(ethylenedioxy)thiophene (1.46 g, 4.78 mmol),

(22) Bauerle, P.; Wurthner, F.; Goetz, G.; Effenberger, F. *Synthesis* **1993**, 1099.
(23) Zhu, S.S.; Swager, T.M. *J. Am. Chem. Soc.* **1997**, *119*, 12568.
(24) Zotti, G.; Zecchin, S.; Schiavon, G.; Vercelli, B.; Groenendaal, L.; *Chem. Mater.* **2003,** *15*, 2222.
(25) Zotti, G.; Zecchin, S.; Schiavon, G.; Vercelli, B.; Berlin, A.; Grimoldi, S. *Macromol. Chem. Phys.* **2004**, *205*, 2026.
(26) Zotti, G.; Zecchin, S.; Schiavon, G.; Berlin, A. *Macromolecules* **2001**, *34*, 3889.
(27) Zotti, G.; Zecchin, S.; Schiavon, G.; Berlin, A. *Chem. Mater.* **2002,** *14*, 3607.

18-crown-6 (311 mg, 1.17 mmol), and KCN (2.20 g, 33.87 mmol) in acetonitrile (30 mL) was refluxed for 13 h. The reaction mixture was poured into water and extracted with ether. The organic phase was washed with water, dried (Na2SO4), and the solvent evaporated. Flash chromatography of the residue (silica gel, hexane/ether 7:3) afforded the title compound as an oil (1.15 g, 95% yield). Anal. Calcd for $C_{13}H_{17}NO_2S$: C, 62.16; H, 6.77; N, 5.57%. Found: C, 62.03; H, 6.69; N, 5.51%. ^{1}H NMR ($CDCl_3$): δ 1.37 (m, 4H), 1.66 (m, 4H), 2.34 (t, 2H), 2.65 (t, 2H), 4.16 (s, 4H), 6.13 (s, 1H).

7-[3,4-(Ethylenedioxy)thien-2-yl]heptanoic acid (EC6CA). A mixture of 7-[3,4-(ethylenedioxy)thien-2-yl]heptanenitrile (531 mg, 2.11 mmol) and KOH (2.96 g, 52.74 mmol) in ethanol/water 1.5:1 (50 mL) was refluxed for 9 h. Most of the ethanol was evaporated at reduced pressure, and the solution acidified with HCl, and extracted with CH_2Cl_2. The organic phase was washed with water, dried (Na2SO4), and the solvent evaporated. Flash chromatography of the residue (silica gel, CH_2Cl_2/methanol 97:3) afforded the title compound as an oil (590 mg, 97% yield). Anal. Calcd for $C_{13}H_{18}O_4S$: C, 57.79; H, 6.66%. Found: C, 57.67; H, 6.59%. ^{1}H NMR ($CDCl_3$): δ 1.37 (m, 4H), 1.62 (m, 4H), 2.35 (t, 2H), 2.62 (t, 2H), 4.17 (s, 4H), 6.11 (s, 1H). MS, *m/e* 270 ($M^{\bullet}+$).

7-[5-Bromo-3,4-(ethylenedioxy)thien-2-yl]heptanenitrile. *N*-Bromosuccinimide (176 mg, 0.99 mmol) was added portionwise to a solution of 7-[3,4-(ethylenedioxy)thien-2-yl]heptanenitrile (243 mg, 0.97 mmol) in DMF (10 mL). After 3 h of stirring, water was added and the resulting mixture extracted with ether. The organic phase was washed with water, dried (Na_2SO_4), and the solvent evaporated to give the title compound as a yellow oil which was used without any further purification for the next step. ^{1}H NMR ($CDCl_3$): δ 1.31−1.66 (m, 8H), 2.33 (t, 2H), 2.59 (t, 2H), 4.21 (m, 4H).

7-[3,4:3′4′Bis(ethylenedioxy)-2,2′-thien-5-yl]heptanenitrile. A mixture of 7-[5-bromo-3,4-(ethylenedioxy)thien-2-yl]heptanenitrile (327 mg, 0.99 mmol), 2-(tributylstannyl)-3,4-(ethylenedioxy)-thiophene (513 mg, 1.19 mmol), $PdCl_2(PPh_3)_2$ (catalytic amount), and DMF (15 mL) was heated at 80 °C for 7 h. The reaction mixture was poured into water and extracted with ether. The organic phase was washed with water, dried (Na2SO4), and the solvent evaporated. Flash chromatography of the residue (silica gel, hexane/ether 6:4) afforded the title compound as a white solid (115 mg, 30% yield). Anal. Calcd for $C_{19}H_{21}NO_4S_2$: C, 58.32; H, 5.37; N, 3.58%. Found: C, 58.23; H, 5.27; N, 3.51%. ^{1}H NMR ($CDCl_3$): δ 1.32 (m, 4H), 1.66 (m, 4H), 2.35 (t, 2H), 2.67 (t, 2H), 4.25(m, 4H), 4.32 (m, 4H), 6.25 (s, 1H).

7-[3,4:3′4′Bis(ethylenedioxy)-2,2′-thien-5-yl]heptanoic acid (E2C6CA). This compound was prepared following the same procedure described above for the synthesis of EC6CA, starting from 7-[3,4:3′4′bis(ethylenedioxy)-2,2′-thien-5-yl]heptanenitrile. The title compound was obtained as a white solid (72% yield), mp 125 °C. Anal. Calcd for $C_{19}H_{22}O_6S_2$: C, 55.62; H, 5.36%. Found: C, 55.53; H, 5.29%. ^{1}H NMR ($CDCl_3$): δ 1.39 (m, 4H), 1.65 (m, 4H), 2.37(t, 2H), 2.66 (t, 2H), 4.23 (m, 4H), 4.32 (m, 4H), 6.24 (s, 1H). MS, *m/e* 410 ($M^{\bullet}+$).

2.2. Substrates and Film Formation. ITO/glass electrodes were 1 × 4 cm^2 ITO one-side coated float-glass sheets (20 Ω sq^{-1}, Merck-Balzers). The ITO microstructure consists of grains ca. 100 nm in diameter and 3 nm high (average). The ITO/glass electrodes were cleaned with acetone and dried prior to use.

Gold electrodes for general use were 1 × 4 cm^2 sheets. They were treated for 1 min with hot mixed chromic acid ($K_2Cr_2O_7$ in 96% H_2SO_4) and then carefully washed with Milli-Q-water and dried.

Gold electrodes for microcontact printing were produced on 1 × 4 cm^2 float glass sheets with a root-mean-square roughness of ca. 0.7 nm. The float glass surface was first cleaned with Piranha solution (30% hydrogen peroxide/70% concentrated sulfuric acid) for 2 min (*Caution: Piranha solution reacts violently with organics and must be handled with extreme care.*) then carefully rinsed with Milli-Q water and dried. Subsequently they were covered with 10 nm of evaporated chromium followed by 100 nm of evaporated gold and stored under nitrogen.

PTT films were produced on platinum electrodes by potentiostatic oxidation at 0.60 V of 5 × 10^{-3} M terthiophene in acetonitrile + 0.1 M Bu_4NClO_4 followed by potentiostatic reduction to the undoped state.

T3C6CA, T3CA, T2C6CA, and EC6CA monolayers on ITO electrodes were prepared from acetonitrile (T3C6PA from ethanol and E2C6CA from ethanol−hexane 1:9 vv) in 10^{-3} M concentration for 5 min as previously reported.[19] Millimolar solutions of T3SH in EtOH/CH_2Cl_2 1:1 vv mixture and of T3C6SH in ethanol were used for 16 h in monolayer formation on gold.[10]

2.3. Apparatus and Procedure. Experiments were performed in acetonitrile + 0.1 M Bu_4NClO_4 at 25 °C under nitrogen in three electrode cells. The counterelectrode was platinum; unless otherwise stated the reference electrode was a silver/0.1 M silver perchlorate in acetonitrile (0.34 V vs standard calomel electrode). The voltammetric apparatus (AMEL, Italy) included a 551 potentiostat modulated by a 568 programmable function generator and coupled to a 731 digital integrator.

Electronic spectra were obtained from a Perkin-Elmer Lambda 15 spectrometer; Fourier transform (FT) IR spectra were taken on a Perkin-Elmer 2000 FT IR spectrometer.

FT IR spectra of the polymer films were taken in reflection−absorption mode. IRRAS spectra of layers were taken with a grazing incidence reflection unit (Specac). All spectra were recorded with a 2-cm^{-1} resolution at an angle of incidence of 80° relative to the surface normal. Cycles (10) were run for each spectrum, and weighted subtraction of the background at the end of the series of measurements was applied. No gas purging of the chamber was necessary.

Electrochemical Quartz Crystal Microbalance (EQCM) analyses were performed with a platinum-coated AT-cut quartz electrode (0.2 cm^2), resonating at 9 MHz, onto which the polymers were deposited. The oscillator circuit was homemade, and the frequency counter was Agilent model 53131A.

XPS of monolayers on gold sheets was done using a PHI 5600ci spectrometer with a base pressure of 2 × 10^{-10} mbar (ultrahigh vacuum) and monochromatized Al Kα radiation ($h\nu$ = 1486.6 eV). The binding energy of the gold Au($4f_{7/2}$) line was calibrated to be 84.00 eV. The experimental conditions are such that the full width at the half maximum of the gold Au($4f_{7/2}$) line is 0.70 eV. Spectra were recorded using an electron takeoff angle of 45, 20, and 10° with respect to the sample surface plane.

AFM was performed in contact mode in air at room temperature using a DME DS 95-200 Dualscope STM equipped with contact-mode silicon tips with a nominal tip radius of 10 nm. Topography and friction force images were recorded simultaneously.

2.4. Microcontact Printing. Stamps used for microcontact printing were fabricated by replica molding of Sylgard 184 poly(dimethylsiloxane) (PDMS) elastomer (Dow Corning) against a photoresist master fabricated on a silicon wafer by photolithograpy. The photoresist master consisted of a periodic array of lines having a height of ca. 2 μm, a width of ca. 2 μm, and period of 6 μm. Adsorbate solutions were 1 mM in ethanol. Phosphonated adsorbates were printed on ITO substrates by inking the stamp with a drop of adsorbate solution for ca. 30 s followed by blowing away the excess ink with a dry nitrogen flow. The stamp was then contacted with the ITO surface for ca. 5 min and then gently

Scheme 2

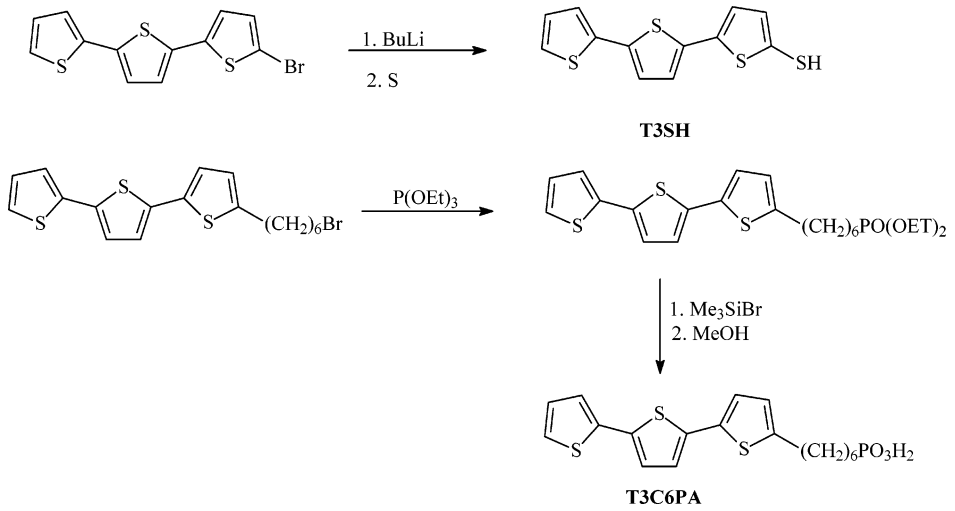

Scheme 3

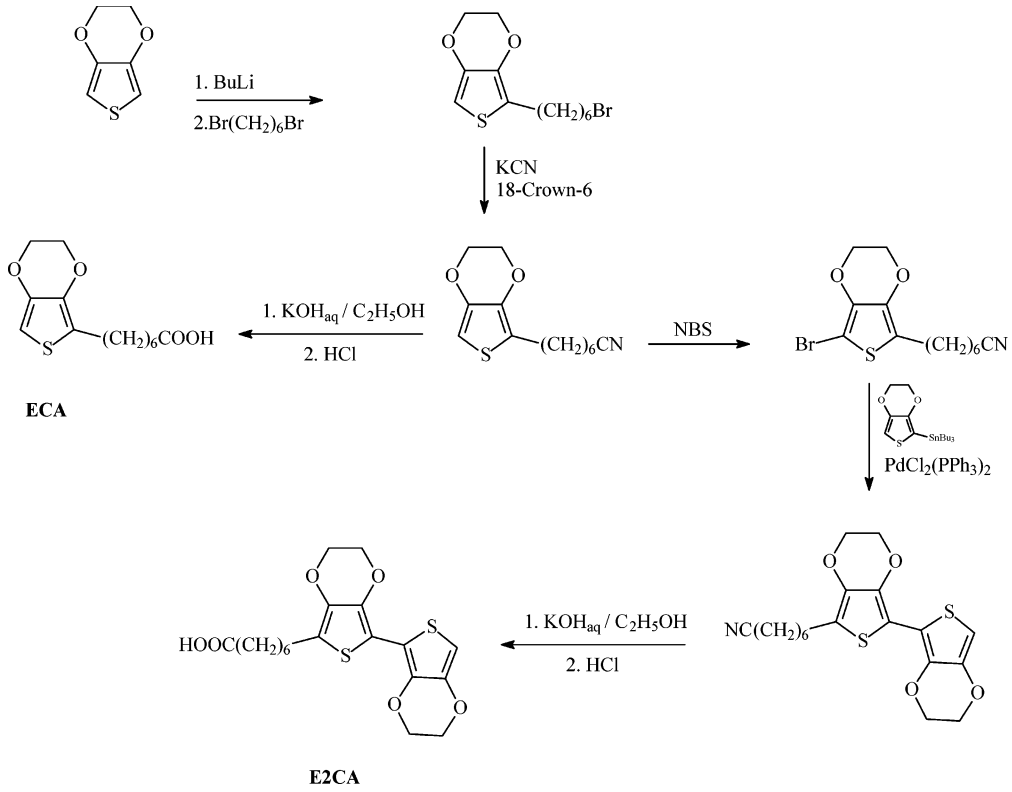

removed. Thiol adsorbates were printed on Au by first soaking a PDMS sheet, acting as ink-pad, in the adsorbate solution for 30 s followed by blowing away of the excess solution. The stamp is then contacted with the ink-pad for 30 s, and printing on Au is performed by contacting the stamp with the Au surface for 30 s. The use of an ink pad in this case was necessary to limit the deposition by evaporation of adsorbates from the recessed, non-contacting, parts of the stamp, which lead to blurring of the patterns.

3. Results and Discussion

3.1. Synthesis of the Compounds. As reported in the Experimental Section, compounds T3CA, T3C6SH, and TPEO were prepared following known procedures, while compounds T2C6CA, T3C6CA, PY, DT, and DP were prepared by us in the context of preceding works.

T3SH was prepared from 5-bromo-2,2′:5′,2″-terthiophene through reaction with BuLi and then with sulfur, as depicted in Scheme 2. In the same scheme, the synthesis we followed for the preparation of T3C6PA is reported. Diethyl 6-(2,2′:5′:2″-terthien-5-yl)hexylphosphonate was hydrolyzed following the method of Rabinowitz.[28] The phosphonate was reacted with trimethylbromosylane and the obtained silyl ester treated with methanol.

The synthetic routes we followed for the preparation of EC6CA and E2C6CA are reported in Scheme 3. 2-(6-Bromohexyl)-3,4-(ethylenedioxy)thiophene, prepared from 3,4-(ethylenedioxy)thiophene through reaction with BuLi and alkylation with 1,6-dibromohexane, was reacted with KCN

(28) Rabinowitz, R. *J. Org. Chem.* **1986**, *51*, 3488.

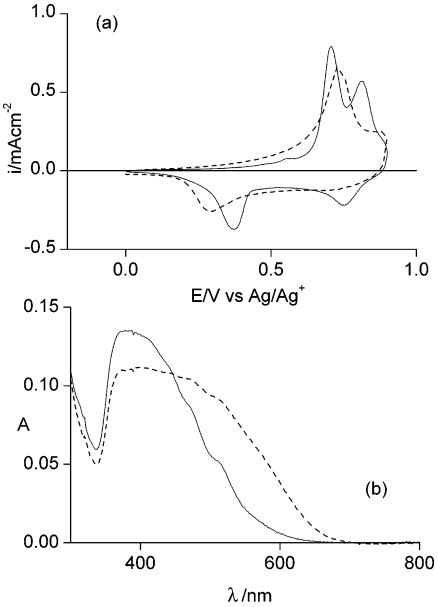

Figure 1. (a) CV of PTT films (solid line) first and (dashed line) last scan in acetonitrile + 0.1 M Bu_4NClO_4. Scan rate: 0.1 V s^{-1}. (b) UV−vis spectra of PTT film (solid line) before and (dashed line) after CV scans. Redox charge: 1 mC cm^{-2}.

and the obtained nitrile hydrolyzed to the corresponding acid. 7[-3,4-(Ethylenedioxy)thien-2-yl]heptanenitrile was bromurated with NBS and the bromo-derivative reacted with 2-(tributylstannyl)-3,4-(ethylenedioxy)thiophene in the presence of $PdCl_2(PPh_3)_2$. Hydrolysis of the obtained nitrile afforded compound E2C6CA.

3.2. Characterization of Polyterthiophene Films. Terthiophene is oxidized with formation of a polymer (PTT) which is in fact the dimer (sexithiophene).[29] CV of PTT film, pristine and after CV cycling (up to 0.9 V at most, to avoid overoxidation), shows the evolution from sexithiophene to dodecathiophene (Figure 1a). The processes at $E_{pa} = 0.70$ V and $E_{pc} = 0.30$ V of the CV-cycled PTT are in fact due to dodecathiophene produced from solid-state dimerization of sexithiophene.[17,18] The evolution is shown also in the UV−vis spectra (Figure 1b).

The redox cycle of pristine PTT is due to two one-electron oxidation processes of the sexithiophene,[17b] whereas the redox cycle of CV-cycled PTT is accounted for by two closely spaced two-electron processes in dodecathiophene (4 electrons per 12 thiophene rings, i.e., 0.33 electron per thiophene ring). We have checked this by EQCM and found that the CV-cycled PTT dodecamer lodges 0.35 electrons per thiophene ring at 0.9 V, in very good agreement with expectations.

3.3. Anodic Coupling to PTT Films. 3.3.1. General Procedure. Polymerization on PTT films was performed as follows. As-deposited PTT-coated electrodes (typically storing a reversible charge $Q_r = 1$ mC cm^{-2}) were immersed in acetonitrile + 0.1 M Bu_4NClO_4 containing the monomer to be coupled. The monomer concentration was 1×10^{-2} M for TPEO and 4×10^{-3} M for PY but was allowed to be lower (10^{-3} M) for DT and DP by their lower oxidation potential. For the pyrroles, 1% H_2O was added to favor polymerization.[30] Repetitive CV beyond 0.8 V, i.e., that of PTT and the monomer oxidation potentials (given in Table 1) were performed at 0.1 V s^{-1}, then the electrode was washed and CV analyzed in a monomer-free solution. The monomer oxidation charge Q_{ox} was always in excess of that of the PTT oxidation charge Q_r, thus ensuring excess of reacting species at the surface.

Table 1. Oxidation Peak Potentials (vs Ag/Ag^+) for Compounds in Solution E_p(s) and as Monolayers E_p(m)

compound	E_p(s)/V	E_p(m)/V
TPEO	1.16	
DT	0.68	
PY	0.72	
DP	0.39	
T3CA	0.81	0.74[a]
T3C6CA	0.65	0.55[a]
T3C6PA	0.60	0.52[a]
T2C6CA	0.80	0.72[a]
EC6CA	1.00	0.80, 1.00[a]
E2C6CA	0.36	0.26, 0.40, 0.56[a]
T3SH	0.78	0.65[b]
T3C6SH	0.66	0.73[b]

[a] ITO. [b] Gold.

It must be kept in mind that, though the homopolymers are soluble, anodic coupling may occasionally produce extra (non-surface-coupled) polymer within the PTT deposit in amounts small but still appreciable. These are eliminated completely by CV cycling under stirring in monomer-free electrolyte.

The dependence of the resulting CV responses on monomer concentration and PTT thickness has been investigated. It was found that the used monomer concentrations were high enough to obtain concentration-independent responses. Thus decreasing the PY or increasing the DP concentration to 2×10^{-3} M did not significantly change the results.

The PTT thickness had to be kept low ($Q_r \leq 1$ mC cm^{-2}, corresponding to a thickness $d \leq 30$ nm) in order to have a response proportional to the PTT amount. For thicker films the process levels off which must be ascribed to a low rate of permeation of the monomer through the PTT matrix.

3.3.2. TPEO and PY. The first CV of the PTT-coated electrode in TPEO solution shows the PTT oxidation leaning on the oxidative process of TPEO. Analogously PTT film oxidation in PY solution appears as a spike over the diffusion-controlled oxidative process of PY.

After CV cycling the CV in monomer-free electrolyte evidences a redox system at $E^0 = -0.2$ V for TPEO (Figure 2a) and $E^0 = -0.05$ V for PY (Figure 3a), attributable to oxidation of both the sexithiophene and the poly(TPEO) or poly(PY) segments.

The total stored charge Q_r increases with the TPEO or PY oxidation charge Q_{ox} attaining a limiting value (Figures 2b and 3b). The maximum reversible charge is 4 (for TPEO) and 5 (for PY) times that of the PTT original layer, which is actually buried in the overall CV response appearing possibly as a round feature at ca. 0.5 V.

Since no polymer is deposited on the bare platinum electrode under the same conditions, the oxidation process

(29) Xu, Z.; Fichou, D.; Horowitz, G.; Garnier, F. *J. Electroanal. Chem.* **1989**, *267*, 339.

(30) Diaz, A.F. *Chem. Scripta* **1981**, *17*, 145.

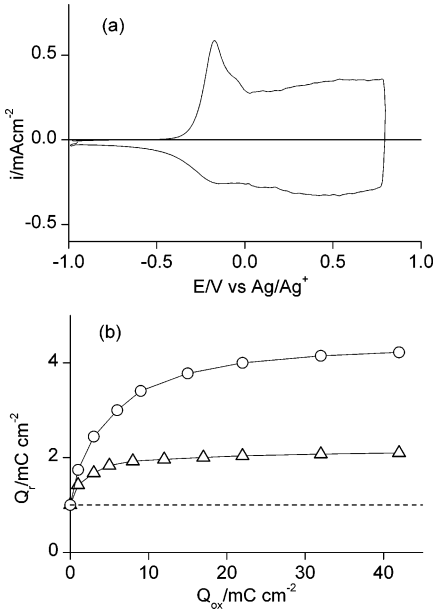

Figure 2. (a) Cyclic voltammogram of TPEO-modified PTT film in acetonitrile + 0.1 M Bu_4NClO_4. Scan rate: 0.1 V s^{-1}. (b) redox charge of TPEO-modified PTT film vs TPEO oxidation charge. (○) pristine and (△) CV-cycled PTT.

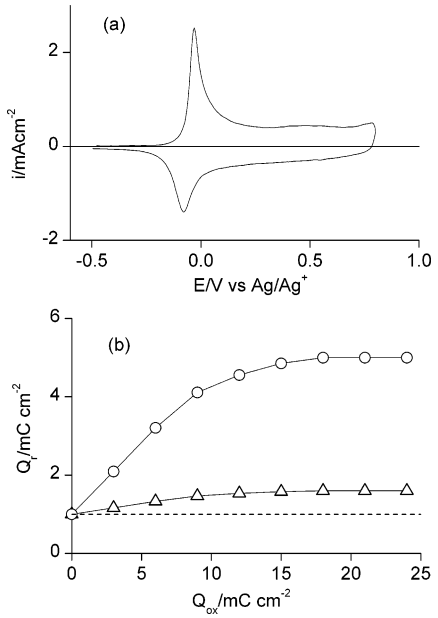

Figure 3. (a) Cyclic voltammogram of PY-modified PTT film in acetonitrile + 0.1 M Bu_4NClO_4. Scan rate: 0.1 V s^{-1}. (b) Redox charge of PY-modified PTT film vs PY oxidation charge. (○) pristine and (△) CV-cycled PTT.

involves coupling of monomers and sexithiophene to insoluble polymers.

From the increase of reversible charge and the electron stoichiometry of 0.35 electrons per thiophene unit (T, see above) and 0.6 electrons per 3,4-ethylenedioxythiophene unit[31] the TPEO component of the copolymer chains results to be formed by ca. 10 TPEO units (T_6-$TPEO_{10}$). Analogously for PY, using the value of 0.5 electrons per pyrrole unit,[31] the composition of the copolymer chains results to be T_6-PY_{17}.

(31) Zotti, G.; Zecchin, S.; Schiavon, G.; Vercelli, B.; Berlin, A.; Dalcanale, E.; Groenendaal, L. *Chem. Mater.* **2003**, *15*, 4642.

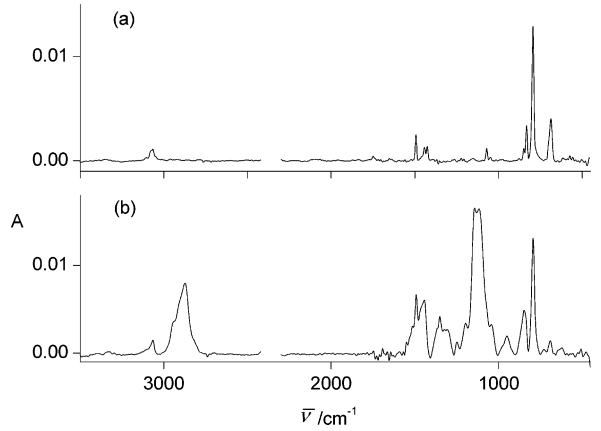

Figure 4. Reflection−absorption FTIR spectra of a PTT-coated platinum electrode (a) before and (b) after TPEO modification.

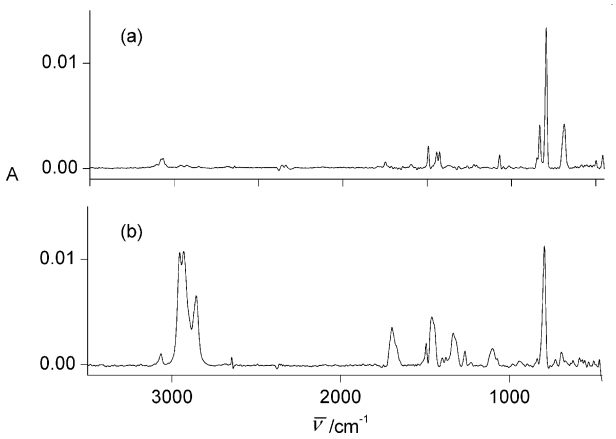

Figure 5. Reflection−absorption FTIR spectra of a PTT film (a) before and (b) after PY modification.

Coupling with the monomer radical cation in the solution likely occurs at the free α positions of sexithiophene radical cation on the electrode surface. In fact CV cycling of PTT to dodecathiophene prior to monomer oxidation decreases strongly (by ca. 50% for TPEO and ca. 85% for PY) its coupling capability (Figures 2b and 3b), thus confirming that the PTT reacting species is the radical cation of the thiophene oligomer.

FTIR confirms the suggested evolution of the PTT deposit with TPEO (Figure 4) and PY oxidation (Figure 5). The spectrum of PTT shows the main bands at 790 and 690 cm^{-1} due to the CH out-of-plane deformation modes of the inner and outer rings respectively, in a 2:1 integrated ratio as in sexithiophene. With coupling to TPEO, new strong bands (mainly at 2900 and 1100 cm^{-1} due to ethylenedioxy units) add to the spectrum (Figure 4b). In the case of PY new strong bands are the methylene bands at 2930, 2860, and 1460 cm^{-1} and bands at 1330 and 1100 cm^{-1}, the latter due to C−N stretching.

The occurred grafting is demonstrated by the fact that in both cases the terminal band at 690 cm^{-1} has dramatically decreased. The persisting aromatic C_β−H stretching band at 3060 cm^{-1} ensures that the thiophene component is present practically unchanged.

Also UV−vis spectroscopy evidences the coupling. The yellowish PTT deposits, showing the maximum at 370 nm and the solid-state vibronic pattern characteristic of sexithio-

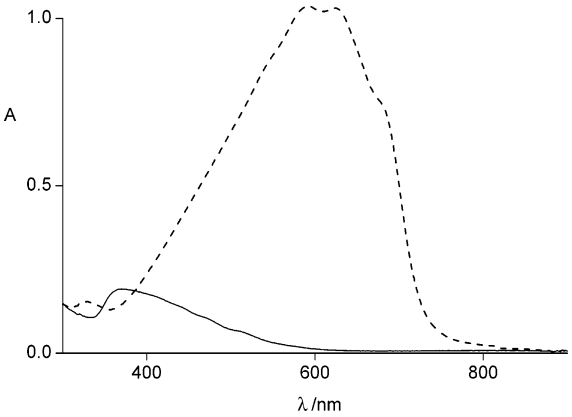

Figure 6. UV-vis spectra of PTT film (solid line) before and (dashed line) after coupling to TPEO.

phene[32] (Figure 6), after TPEO oxidation changes to deep blue with a vibronic structure centered at 600 nm and composed by maxima at 590, 625, and 680 nm. This pattern is the same of analogous 3,4-ethylenedioxythiophene-based polymers investigated previously.[24]

The absorbance has increased by ca. 5 times. From the charge ($Q_r = 1$ mC cm^{-2}, two-electron reversible oxidation) the sexithiophene coverage results to be ca. 5×10^{-9} mol cm^{-2}. From the extinction coefficient (2×10^4 M^{-1} cm^{-1}),[24] the TPEO coverage (in repeat units) corresponds to 5×10^{-8} mol cm^{-2}. It is thus inferred that the sexithiophene molecule is coupled to ca. 10 TPEO units in very good agreement with the coulometrically established stoichiometry.

3.3.3. DT and DP. The PTT and DT oxidation processes occur together at $E_p = 0.7$ V. After 5 CV cycles up to 0.8 V, the filmed electrode shows in monomer-free electrolyte a CV response at $E^0 = 0.0$ V, due to poly(DT),[26] followed by the response of dodecathiophene. The charge of the poly(DT) component does not exceed 30% of the total reversible charge and is not increased with further DT oxidation.

It is therefore inferred that coupling of sexithiophene to DT occurs in competition with its self-dimerization. From the partition of the reversible charge and the electron stoichiometry of 0.35 electrons per thiophene unit for dodecathiophene and 0.5 electrons per DT unit[33] the copolymer may better be considered as a ca. 1:1 blend of dodecathiophene and sexithiophene-DT brushes (T_6-DT_n, $n = 7$).[26]

DP behaves similarly with DT. In the coupling process, the oxidation of DP at $E_p = 0.39$ V is followed by the PTT oxidation at $E_p = 0.67$, and after 5 CV cycles up to 0.8 V, the filmed electrode shows in monomer-free electrolyte a CV response at $E^0 = 0.15$ V, due to poly(DP)[27] and that of dodecathiophene. In this case the charge of the poly(DP) does not exceed 10% of the total reversible charge. Thus coupling of DP with sexithiophene occurs at a very low extent.

3.3.4. Potential Mismatch and Coupling Reactivity. The key step in the construction of the composite films and layers is the heterocoupling of oligomers with different length and nature. The mechanism of electropolymerization, that involves the formation of the carbon−carbon bond by reaction between two radical cations, has been deeply investigated and clarified in the recent past.[34] First of all, the contemporary production of radical cations on the electrode surface (for the PTT film) and in the solution close to the electrode (for the monomer in solution) is required for heterocoupling. Thus the process is favored by a low difference of oxidation potentials (low potential mismatch) of the surface and the solution components. The second factor controlling the coupling process is the reactivity to coupling of the produced radical cations. In fact it appears that in the present case the factor controlling the coupling process is the second one since reactivity is higher for the monomeric (TPEO and PY) than for the dimeric (DT and DP) monomers.[34a−b]

The TPEO and PY components of the copolymer chains result to be constituted by ca. 10 and 18 PY units, respectively. Since poly(TPEO) and poly(PY) are produced electrochemically (under similar conditions) with a degree of polymerization of ca. 6[24] and 13 units,[25] respectively, it appears that the results with PTT are in line with the homogeneous coupling, with a suggested coupling to both the free ends of the sexithiophene chains.

It could be surprising that TPEO polymerizes onto PTT given that the oxidation redox potential of PTT (0.5 V) is much lower than the oxidation potential of TPEO (1.16 V). It is possible that the strong positive shift of PTT oxidation (due to the hysteretic separation of forward and backward CV potentials) moves it close to TPEO oxidation so that a kinetically favorable situation may be the reason of the successful copolymerization.

3.4. Electrochemistry of Adsorbates in Solution. Though we are mainly interested in their adsorbed state, here we summarize the electrochemistry in solution of the thiophene adsorbates. The electrochemical behavior of bithiophene T2C6CA and terthiophene T3C6CA was reported previously.[19] Peak potentials for all monomers 10^{-3} M in acetonitrile + 0.1 M Bu_4NClO_4 (T3C6PA is only slightly soluble, ca. 10^{-4} M) are given in Table 1.

The CVs of T3SH and T3CA show the irreversible oxidation peak at E_p values higher than for T3C6SH and T3C6CA due to the close proximity of the electronwithdrawing substituent and the terthiophene moiety. Continuous cycling produces the deposition of the dimer with redox process and maximum absorption (e.g., 435 nm for T3CA) analogous to those observed previously for T3C6CA dimer (430 nm).[19] For comparison sexithiophene absorbs at 432 nm.[35]

The CV of EC6CA shows its irreversible oxidation peak at Ep = 1.00 V, i.e., close to that of 3,4-ethylenedioxythio-

(32) Fichou, D.; Horowitz, G.; Xu, Z.; Garnier, F. *Synth. Met.* **1992**, *48*, 167.
(33) Zotti, G.; Zecchin, S.; Berlin, A.; Schiavon, G.; Giro, G. *Chem. Mater.* **2001**, *13*, 43.
(34) (a) Waltman, R.J.; Bargon, J. *Tetrahedron* **1984**,*40*, 3963. (b) Waltman, R. J.; Bargon, J. *Can. J. Chem.* **1986**, *64*, 76. (c) Andrieux, C.P.; Audebert, P.; Hapiot, P.; Saveant, J.M. *J. Phys. Chem.* **1991**, *95*, 10158. (d) Audebert, P.; Catel, J.M.; LeCoustumer, J.; Duchenet, V.; Hapiot, P. *J. Phys. Chem.* **1995**, *99*, 11923. (e) Guyard, L.; Hapiot, P.; Neta, P. *J. Phys. Chem.* **1997**, *101*, 5698. (f) Audebert, P.; Catel, J.M.; Duchenet, V.; Guyard, L.; Hapiot, P.; LeCoustumer, J. *Synth. Met.* **1999**, *101*, 642.
(35) Chosrovian, H.; Rentsch, S.; Grebner, D.; Dahm, D.U.; Birckner, E.; Naarmann, H. *Synth. Met.* **1993**, *60*, 23.

Table 2. Oxidation Charge (μC cm^{-2}) for SA Monomer Films (Q_{ox}) and Polymer Brush Electrodes (Q_r)

monomer	Q_{ox}	Q_r (TPEO)	Q_r (PY)
T3CA	40	40	80
T3C6CA[a]	20	20	40
T3C6PA[a]	130	130	140
T3SH	140[a]	130	140
T3C6SH	140[a]	130	140
T2C6CA	30	10	15
EC6CA	30	0	0
E2C6CA	35	10	45

[a] Measured at 1 V switching potential.

phene,[36] with a peak current corresponding to a two-electron oxidation process. The two-electron stoichiometry is confirmed by exhaustive electrolysis which produces nonelectroactive products in solution, probably arising from water attack of the one-electron-oxidized (radical cation) terminal α position and subsequent further one-electron oxidation. Degradation occurs as in the case of T2C6CA[19] due to a higher reactivity in reactions alternative to coupling, such as proton loss from the produced radical cation.

The CV of E2C6CA shows its irreversible oxidation peak at $E_p = 0.36$ V, a voltage lower than for EC6CA and comparable with that of bis-3,4-ethylenedioxythiophene.[37] No solid dimer film was deposited, but dimer was produced in the bulk by electrolysis.

These results indicate that oxidative degradation is a serious obstacle to coupling unless terthiophene or bis-3,4-ethylenedioxythiophene oligomeric ends (or longer oligomers) are used.

3.5. Electrochemistry of Monolayers. 3.5.1. General Procedure and Results. The SA electrodes were tested in acetonitrile + 0.1 M Bu_4NClO_4 with a single CV cycle at a scan rate of 0.1 V s^{-1} up to 1.0 V. The irreversible oxidation charges Q_{ox} involved in this CV cycle for the investigated monolayers are summarized in Table 2.

The monolayers are irreversibly oxidized at E_p values given in Table 1. From the table, a general 0.1 V negative shift of E_p from the value for the compound in solution is observed. This result may be attributed to stabilization of the oxidized monolayer at densely covered sites.

The CV are broad, and on ITO they may show multiple peaks which often merge into a single sigmoidal response. We attribute this result to the presence of different coordination sites on ITO. It appears that the adsorption occurs in general at two different sites of the ITO surface, creating domains of strongly interacting and noninteracting molecules, as previously observed for hexylferrocene phosphonate.[38] The interaction, which may be identified as the well-known π-dimerization of oligothiophene radical cations,[39] favored by the parallel disposition of the oligothiophene chains, is the most likely cause of CV peak broadening.

3.5.2. Monolayers on ITO. The T3CA monolayers on ITO are irreversibly oxidized (Figure 7a) at $E_p = 0.74$ V,

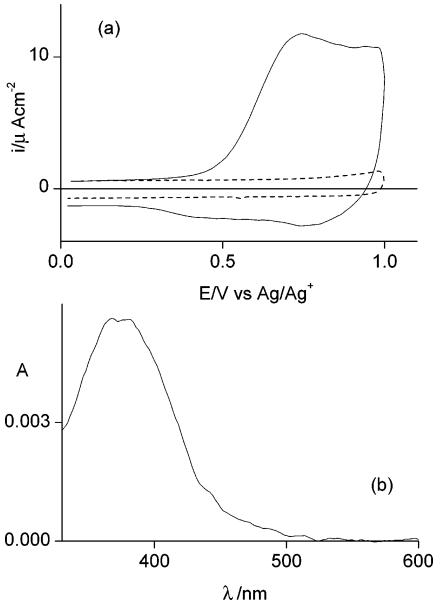

Figure 7. (a) Cyclic voltammogram in acetonitrile + 0.1 M Bu_4NClO_4 and (b) UV−vis spectrum of T3CA-modified ITO. Scan rate, 0.1 V s^{-1}; oxidation charge, 40 μC cm^{-2}.

i.e., a potential higher than for T3C6CA (0.55 V) similarly with the results in solution. The passage of ca. 40 μC cm^{-2}, i.e., twice that of T3C6CA, indicates a higher coverage which may be due either to a stronger link with the surface or to stronger lateral interactions among terthiophene moieties.

From the charge Q_{ox} and with the assumption that the process is a two-electron one, as for the oxidation of EC6CA in solution (see above), the coverage degree for T3CA and T3C6CA is 2×10^{-10} and 1×10^{-10} mol cm^{-2}, the latter in agreement with that measured for the hexylferrocene analogue.[40]

The UV−vis spectra of T3CA (Figure 7b) and T3C6CA monolayers show a maximum absorption at 375 and at 360 nm, respectively, in agreement with the values for the monomers in solution. For T3CA the absorbance of 5×10^{-3}, given $\epsilon = 2 \times 10^4$ M^{-1} cm^{-1} and considering that SA occurs at the same level on both sides of the ITO/glass electrode,[24] allowed to evaluate the degree of coverage as ca. 1.2×10^{-10} mol cm^{-2}. Despite the rough assumption that the values obtained in solution are applicable to possibly oriented films, this value is in acceptable agreement with the electrochemical one.

The T3C6PA monolayers on ITO are irreversibly oxidized with the passage of ca. 130 μC cm^{-2} (ca 6×10^{-10} mol cm^{-2}), i.e., 6 times that of T3C6CA. The higher coverage is due to the stronger link of the phosphonate with the surface already observed for hexylferrocene phosphonate.[38] The UV−vis spectrum confirms the denser coverage since it shows a maximum absorption at 350 nm with an absorbance of 20×10^{-3} corresponding to a degree of coverage of ca. 5×10^{-10} mol cm^{-2}.

3.5.3. Monolayers on Gold. SA gold thiolate monolayers from terthiophene disulfide and terthiophene-undecyl disulfide are reported.[10] T3C6SH has been previously used for monolayer formation on platinum.[11]

(36) Dietrich, M.; Heinze, J.; Heywang, G.; Jonas, F. *J. Electroanal. Chem.* **1994**, *369*, 87.
(37) Sotzing, G.A.; Reynolds, J.R.; Steel, P.J. *Adv. Mater.* **1997**, *9*, 795.
(38) Vercelli, B.; Zotti, G.; Schiavon, G.; Zecchin, S.; Berlin, A. *Langmuir* **2003**, *19*, 9351.
(39) Miller, L.L.; Mann, K.R. *Acc.Chem. Res.* **1996**, *29*, 417 and references therein.
(40) Zotti, G.; Schiavon, G.; Zecchin, S.; Berlin, A.; Pagani, G. *Langmuir* **1998**, *14*, 1728.

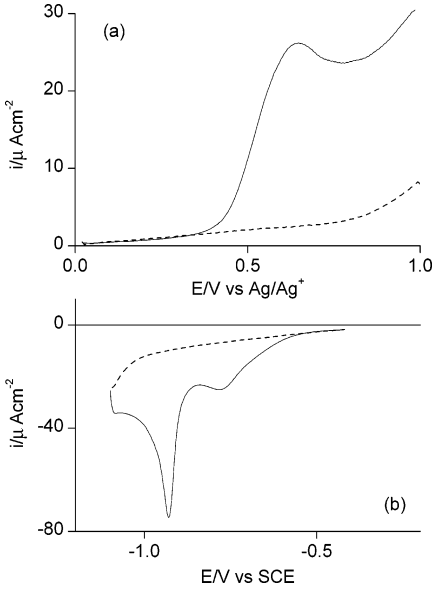

Figure 8. Cyclic voltammogram of T3SH-modified Au: (a) oxidation in acetonitrile + 0.1 M Bu_4NClO_4 and (b) reduction in 0.5 M KOH. Scan rate: 0.1 V s^{-1}.

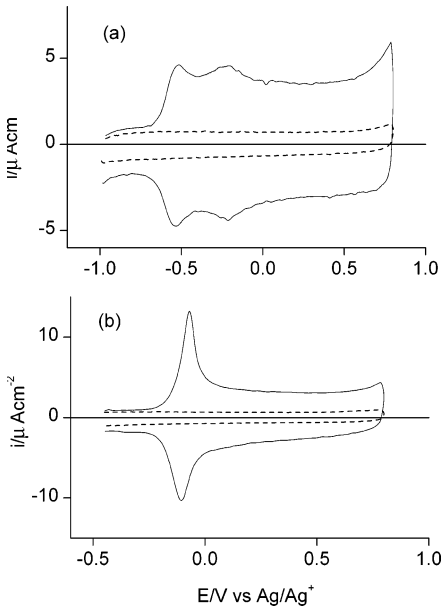

Figure 9. Cyclic voltammogram in acetonitrile + 0.1 M Bu_4NClO_4 of (a) T3CA-modified ITO after TPEO coupling and (b) T3C6CA-modified ITO after PY coupling. Scan rate: 0.1 V s^{-1}.

The T3SH and T3C6SH monolayers on gold are irreversibly oxidized at E_p = ca. 0.70 V (Figure 8a) with the passage of ca. 140 μC cm^{-2} (ca 6 × 10^{-10} mol cm^{-2}), i.e., they form a coverage 4−5 times higher than for the carboxyl adsorbates on ITO and comparable with the phosphonate monolayer (see table). The monolayers of T3SH are also irreversibly reduced in 0.5 M KOH in two peaks at $E_p = -0.75$ and −0.93 V with the passage of ca. 100 μC cm^{-2} (Figure 8b). The latter value is compatible with a full monolayer[41] and compares favorably with the oxidative charge. On the contrary the monolayers of T3C6SH are not reduced in a sharp process but as an ill-defined slope of difficult analysis. This may be accounted for by a more compact structure of the T3C6SH layer, as observed for the terthiophene−undecanethiol layer compared with the terthiophene−thiol layer.[10]

3.6. Anodic Coupling to Monolayers. 3.6.1. General Procedure and Results. Polymerization on the SA electrode was performed under the same conditions used for the PTT-coated electrodes. The SA electrodes were immersed in the solution of the monomer to be coupled (with the same concentrations used for PTT) and a single CV cycle was run at a scan rate of 0.1 V s^{-1} CV up to 0.8 V (1.1 V for TPEO). Then the electrode was carefully washed with acetonitrile and CV analyzed in a monomer-free solution at a scan rate of 0.1 V s^{-1} up to 0.8 V. The reversible charges involved in the CV cycles are summarized in Table 2.

Also in this case the monomer oxidation charge was in excess of that of the surface oxidation charge (1−5 mC cm^{-2} vs 20−40 μC cm^{-2}). Slight excess polymer on the ITO surface after washing was eliminated completely by previous CV cycling under stirring in the monomer-free electrolyte.

CV treatment of the T2C6CA or EC6CA monolayers in any monomer solution does not produce any significant surface polymerization. It appears that the competing reactivity of the bithiophene or 3,4-ethylenedioxythiophene radical cation with the medium is higher than for terthiophene and bis-3,4-ethylenedioxythiophene, confirming the lower reactivity to self-couple found previously[19] and in this report (see above). At difference the terthiophene and bis-3,4-ethylenedioxythiophene monolayers are active as reported below.

3.6.2. TPEO. CV treatment of T3C6CA and T3CA monolayers in TPEO produces an appreciable polymerization. The CV of the coupled polymer shows its redox process (Figure 9a) with a reversible charge which is attributed to the TPEO component solely since the response of the terthiophene component, which is not observed in the CV, is expected to be positively shifted by the oxidized TPEO component.

A coulometric and spectrometric evaluation of the degree of coverage has been done with the T3CA monolayer. By assumption that the redox charge (40 μC cm^{-2}) is due to TPEO units only and with the electron stoichiometry of 0.6 electrons $unit^{-1}$, the charge corresponds to a coverage of 7 × 10^{-10} mol cm^{-2} (in TPEO units). The UV−vis spectrum recorded in situ (Figure 10) shows in the undoped form the usual multiple feature of poly(TPEO) with $A = 12 \times 10^{-3}$ at 622 nm. From the known extinction coefficient, this corresponds to 6 × 10^{-10} mol cm^{-2}, in very good agreement with the electrochemical result.

TPEO couples also with E2C6CA monolayer but with a lower response (10 μC cm^{-2}).

Coupling TPEO with the T3C6PA monolayer gives a high reversible charge of 140 μC cm^{-2}, which reflects the high coverage of phosphonic acid on ITO. For T3SH and T3C6SH monolayers, a similar response (130 μC cm^{-2}, corresponding to a coverage of 20 × 10^{-10} mol cm^{-2}) is obtained.

It must be mentioned that a strongly adsorbed poly(TPEO) monolayer (ca 40 μC cm^{-2}) is formed on the bare gold, whereas no such monolayer formation is observed on ITO. On the other hand it is well known that thiophene and

(41) Kakiuchi T.; Usui H.; Hobara D.; Yamamoto M. *Langmuir* **2002**, *18*, 5231.

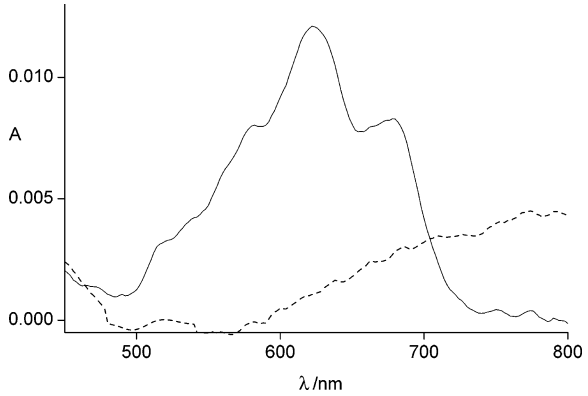

Figure 10. In situ UV−vis spectrum of T3CA-modified ITO after TPEO coupling in acetonitrile + 0.1 M Bu_4NClO_4. (Solid line) undoped form (−1 V) and (dashed line) doped form (0 V). Reversible charge: 40 μC cm^{-2}.

oligothiophenes[42] and 3,4-ethylenedioxythiophene itself[43] are adsorbed on gold. In particular 3,4-ethylenedioxythiophene forms a strongly chemisorbed monolayer with interaction of the π-system and gold.[43] In any case, the adsorbed poly-(TPEO) monolayer is completely removed by hot DMSO, which treatment is on the contrary scarcely effective with the TPEO-coupled thiol monolayers on gold. It is thus clearly shown that in terthiophene-ended thiol layers coupling with TPEO occurs and makes the TPEO layer firmly linked to the terthiophene end, though some noncoupled polymer may be occasionally adsorbed on the primer layer.

3.6.3. PY. After oxidation in PY solution, the T3C6CA monolayer displays the reversible CV response due to poly-(PY) (Figure 9b). Similarly with the TPEO case, the reversible charge (40 μC cm^{-2}) is due to the PY component only, the response of the terthiophene component being not observed in the CV.

Coupling with PY occurs similarly on the T3CA monolayer. The reversible charge up to 0.8 V is 80 μC cm^{-2}, i.e., twice the value with T3C6CA. This result is in line with the amount two times higher of adsorbed T3CA. Oxidation of E2C6CA in PY gives a reversible charge, which is practically the same as for T3C6CA.

Coupling PY on the T3C6PA, T3SH, and T3C6SH monolayers gives a reversible charge of 140 μC cm^{-2}, i.e., 3−4 times that for T3C6CA, which reflects the correspondingly higher coverage of phosphonic acid on ITO and of thiol on gold. By consideration of gold in particular, it must be stressed that, different from poly(TPEO), poly(PY) does not adsorb at all on this metal surface. By assumption once more that the charge is due to PY units only and with the electron stoichiometry of 0.5 electrons unit^{-1}, the reversible charge corresponds to a coverage of 30 × 10^{-10} mol cm^{-2} (in PY units).

3.6.4. DT and DP. CV treatment of the terthiophene-based monolayers in DT or DP solution makes the electrode show in monomer-free electrolyte the CV response of poly(DT)

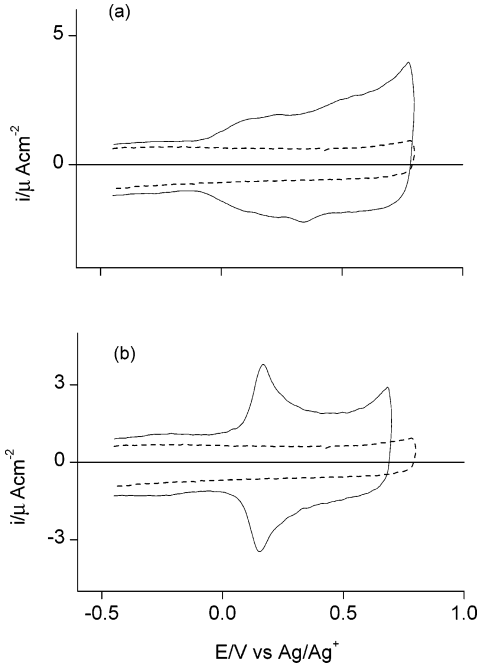

Figure 11. Cyclic voltammogram of T3C6CA-modified ITO after (a) DT and (b) DP coupling in acetonitrile + 0.1 M Bu_4NClO_4. Scan rate: 0.1 V s^{-1}.

at E^0 = 0.10 V (Figure 11a) and of poly(DP) at E^0 = 0.17 V (Figure 11b). In both cases the reversible charge (5−10 μC cm^{-2}) is low. The other monolayers do not appreciably couple with DP or DT.

These results parallel those obtained from PTT (see above). Pyrrole and thiophene dimers are in fact less reactive than the corresponding monomers.[34a−b]

3.6.5. The Brush-Layer Composition and Length. The terthiophene−phosphonate monolayers on ITO as well as the terthiophene−thiolate monolayers on gold have a coverage of ca. 6 × 10^{-10} mol cm^{-2}, i.e., ca 4 times higher than the corresponding carboxyl monolayers on ITO. Thus it is no surprise that their coupling to TPEO or PY gives reversible charges that are 4 times higher than for the carboxyl layers.

In general the degree of coverage of the brush layers is lower (even to a 50% extent) than that of the starting SAMs. By consideration of, e.g., the case of monolayers on gold (ca. 6 × 10^{-10} mol cm^{-2}, see above), the reversible charge after PY coupling corresponds to a coverage of ca. 30 × 10^{-10} mol cm^{-2} (in PY units) and, since bulk polymerization of PY indicates that the PY chain is composed by ca. 12 PY units,[18] the coverage in term of polymer brushes is ca. 3 × 10^{-10} mol cm^{-2}. The loss of coverage may be attributed to either dissolution of the adsorbed molecules due to protons generated by coupling, particularly on the oxide-based ITO surface or to oxidative degradation of the sulfide bond for the thiolates on gold.[44] In any case, if we consider the amount of reversible charge stored in the brush layers (ca. 140 μC cm^{-2}) it results that the layers are still quite thick.

For PY-coupled layers, given that the size of the PY unit is comparable with that of ferrocene (the latter attains a

(42) (a) Matsumura, T.; Shimoyama, Y. *Eur. Phys. J.* **2002**, *7*, 233. (b) Mishina, E.; Miyakita, Y.; Yu, Q.K.; Nakabayashi, S.; Sakaguchi, H. *J. Chem. Phys.* **2002**, *117*, 4016.

(43) Birgerson, J.; Keil, M.; Denier Van der Gon, A. W.; Crispin, X.; Lögdlund, M.; Salaneck, W. R. *Mater. Res. Soc. Symp. Proc.* **2001**, 660.

(44) Everett, W. R.; Welch, T. L.; Reed, L.; Fritsch-Fades, I. *Anal. Chem.* **1995**, *67*, 292.

maximum coverages of 4.5×10^{-10} mol cm^{-2}),[45] the polymer-brush coverage (3×10^{-10} mol cm^{-2}) indicates an extensive yet not completely space-filling coverage.

In the case of TPEO the repeat unit is 5 times bigger than the PY unit thanks to the side ethylenedioxy chain constituted by 50−60 atoms in line. Thus the flexible polyethylenedioxy chains are expected to fill the space available among the adsorbed chains and to extend over the top of the conjugated brush. This conclusion has been confirmed by AFM measurements as reported below.

3.7. IRRAS Spectroscopy of Monolayers. IRRAS spectroscopy was performed on gold modified with T3SH (Au/T3SH) and T3C6SH (Au/T3C6SH). The FTIR spectra of bulk T3C6SH and (more pronouncedly) T3SH are dominated by the strong bands at 790 and 690 cm^{-1} due to the inner and outer thiophene rings. The alkyl chain of T3C6SH adds bands at 2930 and 2860 cm^{-1} due to the methylene antisymmetrical and symmetrical stretching modes.

The bands in the IRRAS spectrum of Au/T3SH are very weak. The 790 cm^{-1} peak is hardly seen in the experimental spectrum although it is by far the strongest peak in the isotropic spectrum (the band at 690 cm^{-1} is not evidenced in IRRAS due to difficult compensation of the CO_2 bending band). This phenomenon is due to the well-known *surface dipole selection rule* for IR spectroscopy at metal surfaces,[46] which only allows modes with vibrational transition dipole moments aligned perpendicular to the metal substrate to interact with the IR beam and appear in the IRRAS spectrum. Thus the transition moment of the 790-cm^{-1} peak must in this case be aligned parallel and the terthiophene chains are as average perpendicularly oriented to the metal substrate.

The IRRAS spectrum of a Au/T3C6SH monolayer, compared with the bulk spectrum of T3C6SH, indicates a substantially unchanged relative intensity of the bands. This indicates that in this case there is no preferential orientation of the molecules on the gold surface.

IRRAS confirms the occurrence of PY coupling. In the IRRAS spectrum of Au/T3SH after PY coupling (Au/T3SH−PY) the PY methylene bands at 2930 and 2860 cm^{-1} and the C−N band at 1100 cm^{-1} show up. At the same time the terthiophene band at 790 cm^{-1} is enhanced, which indicates that a random orientation is introduced by coupling, i.e., the coupled molecules are disordered. In the IRRAS spectrum of Au/T3C6SH−PY, for which the terthiophene molecules were already disordered before coupling, the C−N bands show up and the methylene bands increase in intensity upon coupling to the pyrrole.

3.8. XPS Analysis of Monolayers. Survey XPS spectra of SAMs on gold are shown in Figure 12. The XPS spectrum of Au/T3SH (Figure 12 lower) displays only characteristic peaks from the gold substrate itself and from the C1s, S2s, and S2p core levels of the molecule.[10] An almost identical spectrum is obtained for Au/T3C6SH, i.e., both assemblies appear to be free from contaminations. The thiophene−thiol C1s peak occurs at 285.0 eV; the S2s and S2p binding energies are near 228 and 164 eV. As a whole, the spectra correspond to those reported in the literature.[10]

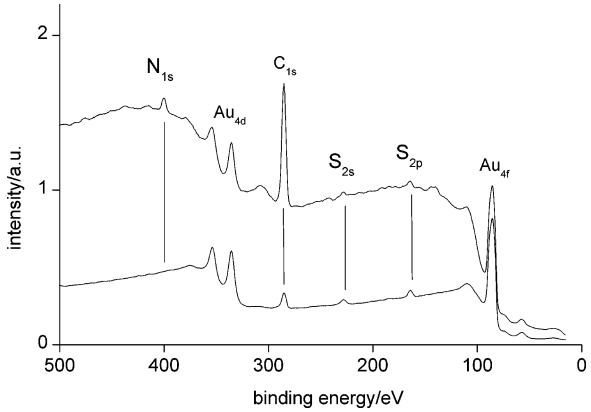

Figure 12. Survey XPS spectra of T3SH-modified Au (lower) before and (upper) after PY coupling. Takeoff angle: 45°.

Table 3. XPS Atomic Percentages and Ratios in T3SH Layers on Gold at 45, 20, and 10° Take-Off Angles

XPS Atomic Percentages

sample	angle	C1s	O1s	Au4f	N1s	S2p	N/S
T3SH	45°	50.3	11.4	25.3	0.0	13.1	0.0
	20°	56.8	14.5	15.0	0.0	13.7	0.0
	10°	63.0	14.5	8.5	0.0	14.0	0.0
T3SH-PY	45°	78.5	7.6	5.8	6.0	2.0	3.0
	20°	84.1	5.1	2.5	6.3	2.1	3.0
	10°	85.0	5.3	1.5	6.1	2.1	2.9

XPS Atomic Ratios

sample	angle	N/S	C/S	C/N
T3SH	45°	0.0	3.8	
	20°	0.0	4.1	
	10°	0.0	4.5	
T3SH-PY	45°	3.0	39.2	13.1
	20°	2.9	40.0	13.3
	10°	3.0	40.0	13.9
calculated		3.0	42.0	14.0

After coupling with PY (Figure 12 upper) a N1s signal at ca. 400 eV shows up and the C1s signal increases strongly its intensity. From the relative intensities (reported in Table 3), it appears that the gold substrate is always shown and that the N/S ratio is constant independently from the takeoff angle. This means that the layer is completely analyzed from base to top.

We have taken the integrated S2p (thiophene and thiol) and N1s (pyrrole) peaks as a measure of the layer composition (see Table 3). The result is that the pyrrole rings are 3 times the sulfur atoms, i.e., that the degree of polymerization of the polypyrrole is 12, in very good agreement with the experimental value of 13 for the bulk polymer.[25] Although some carbon contamination of the samples is in general expected, in this case also the C/S and C/N atomic ratios (see Table 3) are in appreciable agreement with the proposed formulation.

3.9. Microcontact Printing. Microcontact printing has been developed by Whitesides for the preparation of patterns of molecules on bare surfaces by, for example, the transfer of thiols to gold substrates in the contact areas between a soft polymeric stamp and the substrate.[47,48]

(45) Gui, J.Y.; Stern, D.A.; Lu, F.; Hubbard, A.T. *J. Electroanal. Chem.* **1991**, *305*, 37.
(46) Arnold, R.; Terfort, A;; Woll, C. *Langmuir* **2001**, *17*, 4980.
(47) Xia, Y.; Whitesides, G. M.; *Angew. Chem.* **1998**, *110*, 568; *Angew. Chem., Int. Ed. Engl.* **1998**, *37*, 550.

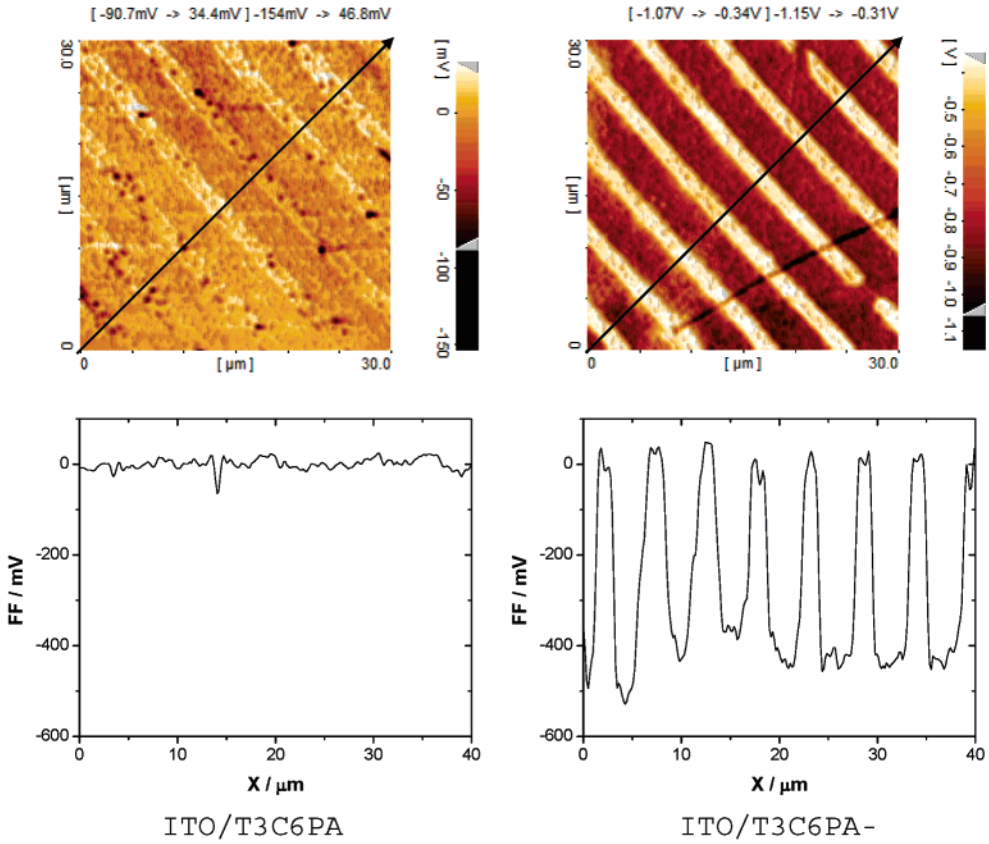

Figure 13. AFM friction force (FF) images (top) and section profiles (bottom) of patterns obtained by microcontact printing of T3C6PA (brighter areas) on ITO (left) before and (right) after coupling with TPEO.

Microcontact printing of phosphonate patterns on ITO and Al_2O_3 surfaces has been only recently reported.[49] Patterns were formed by alkanephosphonic acids and detected by SEM.

Figures 13 and 14 show friction force and topography AFM images, respectively, of T3C6PA patterns printed on ITO. After TPEO coupling the weak primer pattern increases strongly in both the friction force and topography images. The topography of the printed T3C6PA primer pattern is almost invisible, while after coupling with TPEO a film ca. 15 nm thick is obtained on the printed stripes.

The T3C6PA pattern on ITO is strongly enhanced also by PY coupling (not shown). In this case however only friction-force AFM images could be reliably measured. Topography images were very noisy due strong sticking of the AFM tip to the PY film.

No similar results could in general be obtained with the carboxyl adsorbates probably due to their lower surface coverage. As an exception T3C6CA on ITO forms with TPEO polymer brush patterns that are visible both in friction and topography AFM images, whereas no sign of the T3C6CA primer pattern could be detected.

The formation of patterns and their enhancement is observed also on gold. The AFM image of the initial T3C6SH pattern is markedly enhanced (to a height of ca. 5 nm) by coupling to PY.

Given calculated lengths of 0.4 nm for TPEO ring, 0.36 nm for PY ring and 2 nm for the T3C6SH or T3C6PA chains, the expected length for a degree of polymerization of 13 and 6 for poly(PY) and poly(TPEO) (see above) is around 7 and 4.4 nm, respectively. The value measured for T3C6SH−PY (5 nm) is reasonably close to the calculated value whereas the T3C6PA−TPEO brush length (15 nm) is much higher (ca 3 times). Yet if we consider that the PEO chains, which are expected to extend over the top of the conjugated chains, is ca. 7 nm long in an extended linear configuration and that some adsorption of poly(TPEO) is allowed, the observed pattern height is accounted for easily.

4. Conclusions

Anodic coupling of different pyrrole- and thiophene-based monomers with thin polyterthiophene films and oligothiophene-based self-assembled monolayers on ITO and gold electrodes has been investigated. Both monomeric and dimeric pyrrole- and thiophene-based molecules have been tested as monomers for coupling with bithiophene-, terthiophene-, 3,4-ethylenedioxythiophene-, and bi-3,4-ethylenedioxythiophene-tailed monolayers. Carboxyl and phosphonate heads were used to form monolayers on the ITO surface whereas thiol heads were used for gold.

The reactivity to couple, higher for the monomeric than for the dimeric monomers, allows extensive coupling only to the former. By consideration of the coupling site on the

(48) Michel, B.; Bernard, A.; Bietsch, A.; Delamarche, E.; Geissler, M.; Juncker, D.; Kind, H.; Renault, J.P.; Rothuizen, H.; Schmid, H.; Schmidt-Wenkel, P.; Stutz, R.; Wolf, H. *IBM J. Res. Dev.* **2001**,*45*, 697.

(49) (a) Goetting, L.B.; Deng, T.; Whitesides, G.M. *Langmuir* **1999**, *15*,1182. (b) Breen, T.L.; Fryer, P.M.; Nunes, R.W.; Rothwell, M.E. *Langmuir* **2002**, *18*,194.

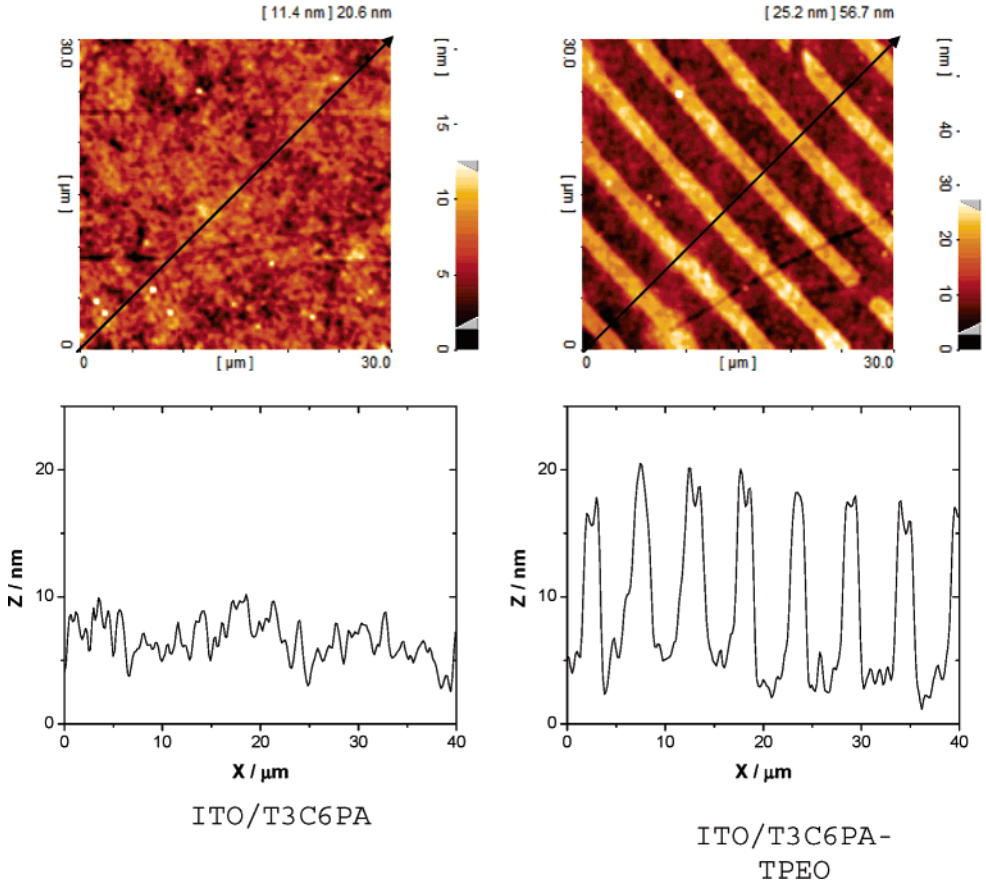

Figure 14. AFM topography images (top) and section profiles (bottom) of patterns obtained by microcontact printing of T3C6PA (brighter areas) on ITO (left) before and (right) after coupling with TPEO.

surface, bithiophene or 3,4-ethylenedioxythiophene tails react with the medium whereas terthiophene and bis-3,4-ethylenedioxythiophene couple efficiently with monomers in solution. The result is that in practice the best combination for heterocoupling is terthiophene-headed monolayers with pyrrole- or 3,4-ethylenedioxythiophene-based monomers.

In this way, nanometer-size layers of polyconjugated polymers with nominally normal orientation of the chain to the surface (polymer-brush electrodes) have been successfully produced.

The first immediate result of this investigation is that microcontact printing on gold and ITO surfaces produces patterns for which heterocoupling yields strong AFM-measured height enhancements, even from nonobserved to clearly evident nanometer-size structures. The long-term result is the possible use of this heterocoupling approach in the realization of organized structures on electrically addressed surfaces, of particular interest in molecular electronics. In this sense the study of the nanoscopic conductive properties of these layers is in progress.

Acknowledgment. The authors thank Dr. Gilberto Schiavon of the CNR for helpful discussions and Mr. S. Sitran of the CNR for his technical assistance. We are also indebted to MIUR-FIRB (Manipolazione molecolare per macchine nanometriche, Project Code RBNE019H9K) and MIUR (Transistori a base di materiali organici e compositi nanostrutturati per impiego come sensori chimici avanzati) for financial support.

CM050300L